Anat Embryol (1999) 199:9–19

ORIGINAL ARTICLE

Sharleen T. Sakai · Masahiko Inase · Jun Tanji

Pallidal and cerebellar inputs to thalamocortical neurons projecting to the supplementary motor area in *Macaca fuscata:* a triple-labeling light microcopic study

Accepted: 29 June 1998

Abstract We investigated the interrelationship between the supplementary motor area (SMA) thalamocortical projection neurons and the pallidothalamic and cerebellothalamic territories in the monkey (*Macaca fuscata*) using a combination of three tracers in a triple labeling paradigm. Thalamic labeling was analyzed following injections of the anterograde tracers, biotinylated dextran amine (BDA) into the internal segment of the globus pallidus (GPi) and wheat germ agglutinin conjugated to horseradish peroxidase (WGA-HRP) into the contralateral cerebellar interpositus and dentate nuclei. In addition, the retrograde tracer cholera toxin subunit B (CTB) was injected into the physiologically identified hand/arm representation of SMA. The tissue was processed sequentially using different chromogens in order to visualize all three tracers in a single section. We found that the SMA thalamocortical neurons occupied a wide band extending from the ventral anterior nucleus pars principalis (VApc) through the ventral lateral nucleus pars oralis (VLo) and the ventral lateral nucleus pars medialis (VLm) and into to the ventral lateral nucleus pars caudalis (VLc) including a portion of ventral posterior lateral nucleus pars oralis (VPLo) and nucleus X. The heaviest CTB labeling was found in VLo with dense plexuses of BDA labeled pallidothalamic fibers and swellings often observed superimposed upon retrogradely labeled CTB cells. In addition, dense foci of cerebellothalamic WGA-HRP anterograde label were observed coinciding with the occasional retrogradely CTB labeled neurons in VLc and transitional zones between VApc, VLo and VPLo. Our light microscopic results suggest that the SMA receives thalamic inputs with afferents largely derived from GPi and minor inputs originating from the cerebellum.

Key words Motor systems · Basal ganglia · Thalamus · Biotinylated dextran amine · WGA-HRP · Cholera toxin subunit B

Abbreviations *CTB* Cholera toxin subunit B · *D* dentate nucleus · *DAB* diaminobenzidine · *F* fastigial nucleus · *GPe* globus pallidus, external segment · *GPi* globus pallidus, internal segment · *I* interpositus nucleus · *ICMS* intracortical microstimulation · *MI* primary motor cortex · *P* putamen · *PBS* phosphate buffered saline · *R* reticular nucleus · *SMA* supplementary motor area · *TBS* TRIS buffered saline · *TMB* tetramethylbenzidine · *VApc* ventral anterior nucleus; pars principalis · *VLc* ventral lateral nucleus, pars caudalis · *VLm* ventral lateral nucleus, pars medialis · *VLo* ventral lateral nucleus, pars oralis · *VPLo* ventral posterolateral nucleus, pars oralis · *WGA-HRP* wheat germ agglutinin-horseradish peroxidase · *X* nucleus X

Introduction

The SMA has been the focus of a number of investigations. A multiplicity of functional roles have been attributed to the SMA including motor preparation (Tanji et al. 1980), bimanual coordination (Brinkman 1984), sequential movement (Roland et al. 1980; Halsband et al. 1993; Tanji and Shima 1994), and postural control (Wiesendanger and Wiesendanger 1985a; reviewed see Tanji 1994). Due to the similarities in behavioral deficits such as akinesia and deficits in sequential movements (Agostino et al. 1992), simultaneous movements (Benecke et al. 1986), and movement initiation (Flowers 1978) observed in Parkinson's patients, the SMA has been strongly linked to the basal ganglia (reviewed Goldberg 1985;

S.T. Sakai (✉)
Department of Anatomy, B517 West Fee,
Michigan State University, East Lansing, MI 48824, USA
e-mail: sakai@com.msu.edu, Tel.: +517-353-8889,
Fax: +517-353-9764

M. Inase[1]
National Institute of Physiological Sciences, Okazaki 444, Japan

J. Tanji
Department of Physiology, School of Medicine, Tohoku University, Sendai 980, Japan

Present address:
[1] Molecular and Cellular Neuroscience Section,
Electrotechnical Laboratory Tsukuba 305, Japan

Tanji 1994). The SMA is reported to be subcortically dependent on the basal ganglia in that its primary thalamic input is from the VLo (Schell and Strick 1984), which in turn receives its input from the GPi (Kuo and Carpenter 1973; Kim et al. 1976; De Vito and Anderson 1982). On the other hand, SMA thalamocortical neurons have also been reported to receive afferents originating from the cerebellum (Wiesendanger and Wiesendanger 1985b; Rouiller et al. 1994). The latter results are intriguing in view of the anatomical and electrophysiological similarities between SMA and the MI which is known to receive massive indirect cerebellothalamic input (Asanuma et al. 1983; Schell and Strick 1984). Both the SMA and MI give rise to corticospinal projections (Murray and Coulter 1981; Dum and Strick 1991) and share similar corticocortical connections (Luppino et al. 1993) such that it has been proposed that the SMA and MI have some functional properties in common (Luppino et al. 1993).

The possibility that thalamic neurons projecting to the SMA receive inputs from the cerebellum is of considerable interest. Wiesendanger and Wiesendanger (1985b) reported transneuronal labeling of cells in the cerebellar nuclei following injections of WGA-HRP into SMA. This result is difficult to interpret since the sites were not electrophysiologically defined prior to injection and were more likely localized to rostral SMA, a region now defined as the pre-SMA (Luppino et al. 1991; Matelli et al. 1991). More recently, on the basis of a multiple labeling study, Rouiller et al. (1994) reported that the cerebellothalamic territories coincided in location with the SMA thalamocortical projection neurons. However, in this study, the relationship of these afferent and efferent projection systems was determined on the basis of comparison between adjacent sections. In order to directly evaluate the interrelationship of the afferent and efferent connectivity, a multiple-labeling paradigm in which all tracers could be visualized in the same histological section is optimal. One drawback of previous multiple-labeling studies was the difficulty in clearly visualizing the different tracers in a single section. Several studies have successfully utilized a double-labeling strategy in order to describe either dual fiber systems (Brandt and Apkarian 1992; Veenman et al. 1992; Dolleman-Van der Weel et al. 1994; Inase et al. 1996; Sakai et al. 1996) or a combination of retrograde and anterograde labels (Bruce and Grofova 1992). Double-labeling studies have typically utilized chromogens yielding a brown reaction product from DAB processing and a blue-black reaction product as a result of either metal intensified DAB or TMB processing. Using this combination of chromogens, we have previously analyzed the organization of the pallidal and cerebellar thalamic territories in the monkey using a double anterograde labeling paradigm (Sakai et al. 1996). Our observations have indicated that both cerebellar and pallidal fibers distributed either as dense single label or as interdigitating patches of double label across individual nuclei of the motor thalamus. Segregation of pallidal and cerebellar afferents occurred in the central core of each nucleus but both afferents were found within transitional zones between nuclei. In addition, we have occasionally observed both cerebellar and pallidal varicose fibers apposed to the same cells in the VLo, which represents a major target of pallidal fibers.

The purpose of the present study was to directly assess the relationship of the cerebellar and pallidal afferents to SMA thalamocortical projection neurons using a triple-labeling paradigm. To achieve this goal, we have combined the previously used double anterograde tracing method with retrograde transport of CTB to mark the thalamic neurons projecting to the SMA. The retrogradely CTB-labeled neurons were visualized by using a new purple chromogen marketed by Vector Laboratories as VIP (Zhou and Grofova 1995). The use of this combination of tracers allowed the black and brown anterograde labels to be distinguished from purple CTB retrogradely labeled cells. Moreover, due to sequential histochemical processing, the three labels were observed in the same section rather than the more common comparison of separately retracted adjacent sections.

Materials and methods

Experiments were performed on three Japanese monkeys (*Macaca fuscata*) weighing between 4.1 and 4.9 kg. Each animal was initially anesthetized by an intramuscular injection of ketamine hydrochloride (10 mg/kg) followed by an intraperitoneal injection of sodium pentobarbital (30 mg/kg). Under aseptic surgical conditions, the skull was exposed and two stainless steel tubes were affixed to the frontal and occipital bones using dental acrylic. The exposed skull was then covered with a 1–2 mm layer of dental acrylic and the animal was allowed to recover. This work was conducted in compliance with the N.I.H. guide for the care and use of laboratory animals.

One to two days following the surgery, the animals were anesthetized with ketamine hydrochloride (10 mg/kg I.M.) and placed in a primate chair. A glass insulated Elgiloy alloy microelectrode (0.8–1.5 µM at 333 Hz) was introduced into the brain at an angle of 45–50° lateral from vertical in order to avoid the overlying thalamus in approaching GPi. A characteristic pattern of spontaneous activity generated from the internal capsule, caudate and putamen provided the guidance necessary for targeting the GPi. The GPi cells were characterized by high frequency spontaneous discharge (DeLong 1971). This activity pattern was utilized in order to define the boundaries of the nucleus prior to the injections of BDA. Following this identification of GPi, a 1.0 µl Hamilton syringe was advanced to the same location using stereotactic coordinates and one to three pressure injections of 0.5–1.0 µl 10% BDA (Molecular Probes, Eugene, Ore.) diluted in 10 mM phosphate buffer pH 7.24 were made into different rostrocaudal portions of GPi.

Six days later, the animals were re-anesthetized with ketamine hydrochloride (10 mg/kg I.M.) and the SMA was mapped using intracortical microstimulation (ICMS). Typically, the threshold for evoking contralateral movement ranged from 20–40 µA with stimulation consisting of trains of 22 cathodal 200 µs pulses applied at 333 Hz. The rate of train presentation was at intervals of 5 s or less. A glass micropipette (tip diameter: 50–100 µm) cemented to a 1.0 µl Hamilton syringe was lowered to a depth of up to 5.0 mm and two pressure injections of up to 1.0 µl of 1% CTB (Sigma) were made into the physiologically identified hand/arm representation of SMA. The CTB was injected at a rate of 0.1 µl per two min. Following the injections, the pipette was left in place for 15 min prior to withdrawal from the cortex. The bone flap was replaced and cemented in place with dental acrylic.

The next day, the animals were re-anesthetized and the bone overlying the occipitoparietal cortex was removed. A microelectrode was introduced into the brain passing vertically through the occipitoparietal cortex, the tentorium cerebelli and into the cerebellum. The cerebellar nuclei were defined electrophysiologically

by their characteristic high amplitude, high frequency spontaneous activity. A series of three to five pressure injections of 0.3–0.5 µl 2.5% WGA-HRP (Toyobo, Japan) were made using a 1.0 µl Hamilton syringe into different rostrocaudal levels of the dentate and interpositus nuclei.

Three days later, the animals were deeply anesthetized with sodium pentobarbital (60 mg/kg) and perfused intracardially with warm PBS, followed by 4% paraformaldehyde, 0.01 M sodium periodate, 0.075 M lysine in phosphate buffer followed by cold 10% and 30% sucrose in phosphate buffer. The brain was removed immediately, photographed, blocked in the coronal plane and immersed in 30% sucrose in phosphate buffer for 2–3 days. Brains were frozen-sectioned at 50 µm thick. Four series of adjacent sections were treated for: HRP histochemistry only, both HRP and BDA histochemistry, HRP, BDA and CTB immunohistochemistry and lastly, a Nissl reference series.

HRP histochemistry

Sections treated for HRP were reached using TMB as the chromogen and ammonium molybdate (Olucha et al. 1985) and stabilized in DAB (Rye et al. 1984). Briefly, sections were rinsed in 0.1 M phosphate buffer (pH 6.2) and incubated in a solution of 0.25% ammonium molybdate and 0.005% TMB in 0.1 M phosphate buffer (pH 6.2) and 0.003% hydrogen peroxide. Sections were incubated overnight at 4° C and then stabilized in a solution of 0.1% DAB, 0.002% cobalt chloride and 0.003% hydrogen peroxide in 0.1 M phosphate buffer (pH 7.4) for 3–5 min. Following a brief rinse in phosphate buffer, sections processed for HRP only were mounted onto slides, dried and counterstained with neutral red. The sections to be processed for BDA and/or CTB were rinsed in 0.1 M phosphate buffer (pH 6.2).

BDA histochemistry

To reveal the BDA, we followed the protocol of Veenman et al. (1992) with minor modifications. The sections were rinsed in 0.1 M phosphate buffer (pH 7.4) and incubated in a 1:500 or 1:50 dilution of avidin-biotin-peroxidase complex (Vector ABC Elite kit, PK 6100) for 2 h. Sections were rinsed in the same phosphate buffer, transferred to TBS and reacted in 0.1% DAB/0.04% ammonium chloride/0.2% β-D glucose and glucose oxidase for 10–20 min. The double reacted HRP and BDA sections were then mounted onto slides, dried, and counterstained with neutral red. The sections to be processed for CTB were rinsed in TRIS buffer.

CTB immunohistochemistry

The final series of sections were reaced for CTB according to the method of Bruce and Grofova (1992). The sections were rinsed in 0.04% Triton X in TBS and blocked in 3.0% normal rabbit serum. They were incubated with gentle agitation in a 1:5000 dilution of goat anti-choleragenoid (List Biological Labs) in TBS with 0.04% Triton X at 4° C for 60 h. The sections were then washed in 0.02% Triton X in TBS and incubated in a 1:200 dilution of biotinylated anti-goat IgG (Vector ABC kit PK 4005) in TBS with 0.02% Triton X. Following additional TBS rinses, the sections were incubated in a 1:1000 dilution of avidin-biotin-peroxidase complex for 2 h and rinsed in 0.02% Triton X in TBS. Prior to using Vector VIP substrate kit (Vector Laboratories, SK 4600), the sections were washed in PBS pH 7.5. The VIP solutions were diluted according to manufacturer instructions in 0.01 M PBS (three drops of each vial for 5 ml of VIP solution). Sections were incubated for 5–15 min, rinsed in distilled water, mounted on slides, dried, cleared in xylene and coverslipped. Control CTB sections were reacted in the same way but were not incubated in the primary antisera. The technical protocol is summarized in Fig. 1.

The location and extent of the injection sites were analyzed using a low magnification projection system. The dense core and halo of the WGA-HRP and BDA injections were drawn in relation to the adjacent structures. The CTB cortical injection sites and ICMS data were reconstructed into a somatotopic map for each animal. The thalamic distribution of the BDA, WGA-HRP and CTB labeling was analyzed and drawn using an Olympus microscope. The delineation of thalamic nuclei was based on cytoarchitectonic analysis of the adjacent Nisl-stained sections using the criteria and nomenclature derived from Olszewski (1952), Kusama and Mabuchi (1970) and Asanuma et al. (1983).

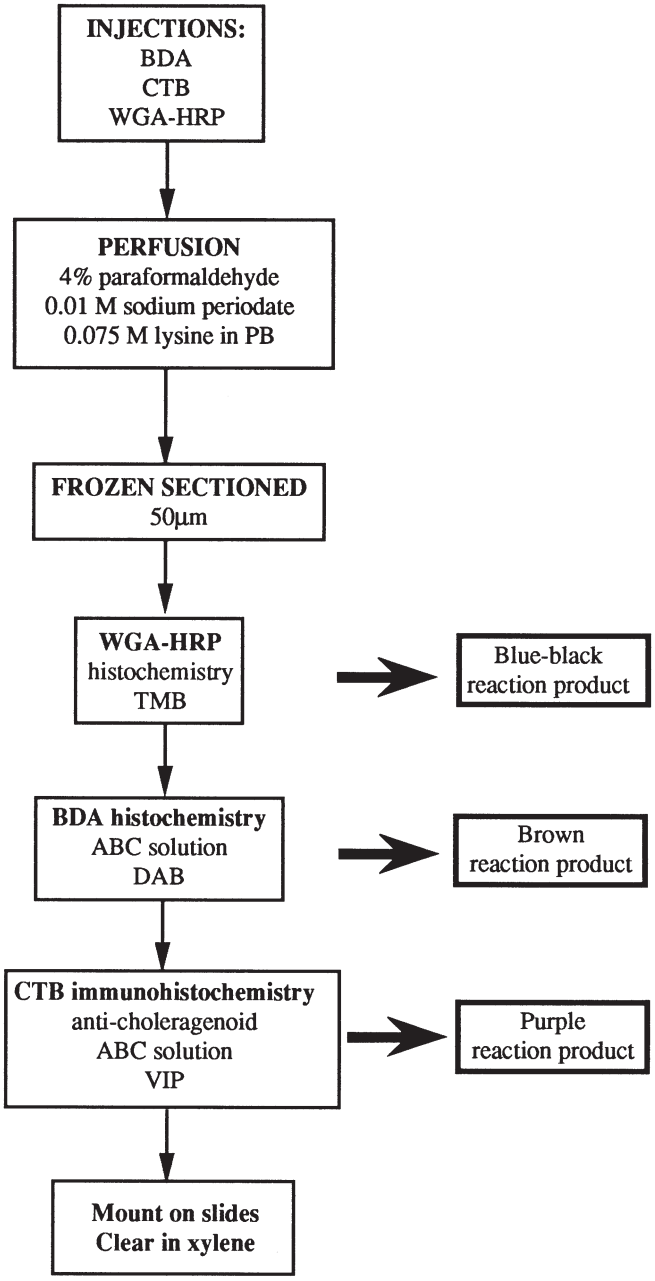

Fig. 1 Flow chart summarizing the triple-labeling protocol

Results

Injection Sites

We successfully injected all three target structures in three cases. The major difference across these cases was

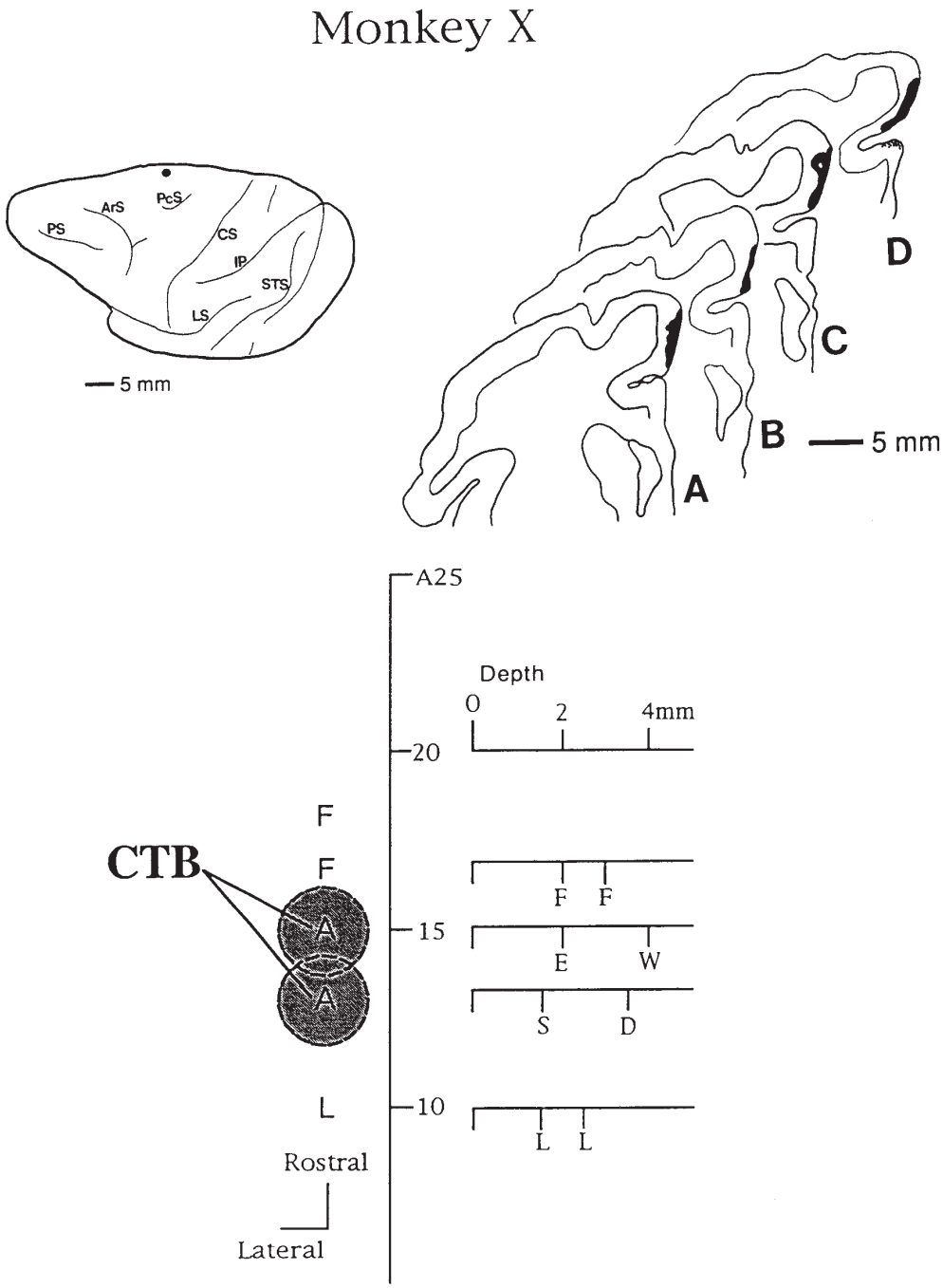

Fig. 2 The CTB injection site into the SMA in monkey *X*. The *upper left panel* shows a lateral view of the cerebral hemisphere showing the relative location of the injection site (*ArS* arcuate sulcus, *CS* central sulcus, *IP* intraparietal sulcus, *LS* lateral sulcus, *PcS* precentral sulcus, *PS* principal sulcus, *STS* superior temporal sulcus). The *upper right panel* shows a rostrocaudal series of sections through the injection site. The *lower panel* shows a schematic representation of the results obtained from intracortical microstimulation of the SMA. The anterior/posterior levels indicated by the center scale bar are in accordance with the atlas of *Macaca fuscata* by Kusama and Mabuchi (1970). For each electrode penetration, the microstimulation results are noted by one of the following abbreviations: *A* arm, *F* face, *E* elbow, *W* wrist, *S* shoulder, *D* digits, *L* leg. The CTB injections into the hand/arm representation are indicated by *shaded circles*

the extent to which the target structures were completely filled with the tracers. Although a difference in the density of labeling was observed, the general distribution of the three labels was similar across all three cases. Therefore, we will present the findings from a single representative case.

The injection sites from monkey *X* are shown in Figs. 2, 3. The SMA was mapped using ICMS and the forelimb/arm representation was identified (Fig. 2). The two CTB injections made into this site were confined to the mesial surface of the hemisphere and consisted of a light purple halo surrounded the needle tracks. The injections into GPi and the cerebellum are shown in Fig. 3. The BDA injections into GPi consisted of a brown halo surrounding darkly stained needle tracks and almost completely filled the GPi with the exception of its most ventromedial aspect (Fig. 3). Although the BDA spread along the needle track into the P and GPe, it is unlikely that this diffusion contributed to ventral thalamic labeling since there are no known projections from these nuclei to the ventral thalamus. A total of six closely spaced WGA-HRP injections made into the contralateral cerebellum resulted in a large blue/black halo completely encompassing the dentate nucleus and much

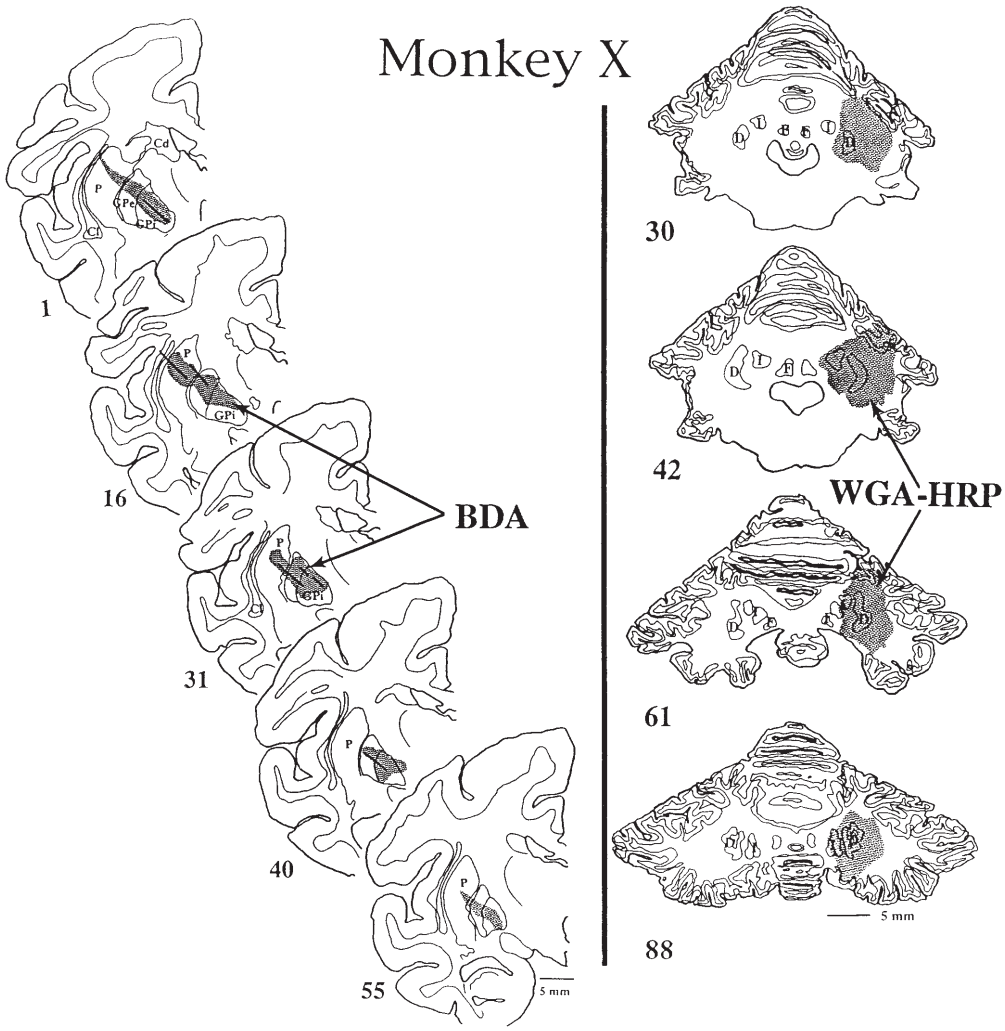

Fig. 3 The *left panel* shows a series of coronal sections through the BDA injection sites into the GPi. *Stippling* indicates the maximal extent of the three BDA injections. The *right panel* shows line drawings of a coronal series through the cerebellar injections sites. *Stippling* indicates the maximal extent of the WGA-HRP injections. These injections include the dentate nucleus and most of the interpositus nucleus

of the interpositus nucleus (Fig. 3). However, the most rostral part of the interpositus nucleus was not injected in case *X*.

Distribution of SMA thalamocortical cells compared to the cerebellothalamic and pallidothalamic projections

We have previously described the detailed relationship between the distribution of the cerebellothalamic and pallidothalamic projections (Sakai et al. 1996). Briefly, we have found that the cerebellothalamic and pallidothalamic territories generally occupy separate thalamic regions but that individual thalamic nuclei receive differential patchy input from both afferent sources. We have found that the central core of individual thalamic nuclei receive one afferent source. However, transitional regions between adjacent nuclei received interdigitating and occasionally, overlapping inputs from both afferent sources. The present description primarily focuses on the distribution of the SMA projection neurons and the relationship of this distribution to the cerebellothalamic and pallidothalamic projections.

The retrograde tracer CTB was visualized using the commercially available Vector VIP chromogen that produces a purple reaction product. The cell somata and proximal dendrites and sometimes, distal dendrites are stained an intensely deep purple to violet color (Figs. 4D–F, 5D–F). Retrogradely labeled CTB cells were distributed as a wide band extending from the most rostral to mid-regions of the thalamus. The band of labeled cells occupied the rostrolateral thalamus including VApc and the VLo. At a slightly more caudal thalamic level, labeled cells were largely found in VLo and VApc with scattered cells in the VPLo (Figs. 4A, D, E, 5A, D, E, 6 section 52). At a more caudal thalamic level as shown in Fig. 5 section 64, the band of labeling in VLo extended medially into the VLm. A few labeled cells were found in VPLo and the VLc. At more caudal thalamic levels, the density of cell labeling decreased as the band of labeling shifted medially. At this level, the greatest density of labeled cells was found in VLo and scattered cells were found in VPLo, VLc and X.

The distribution of the SMA thalamocortical neurons labeled with CTB primarily coincided with the distribution of the pallidothalamic projections visualized with

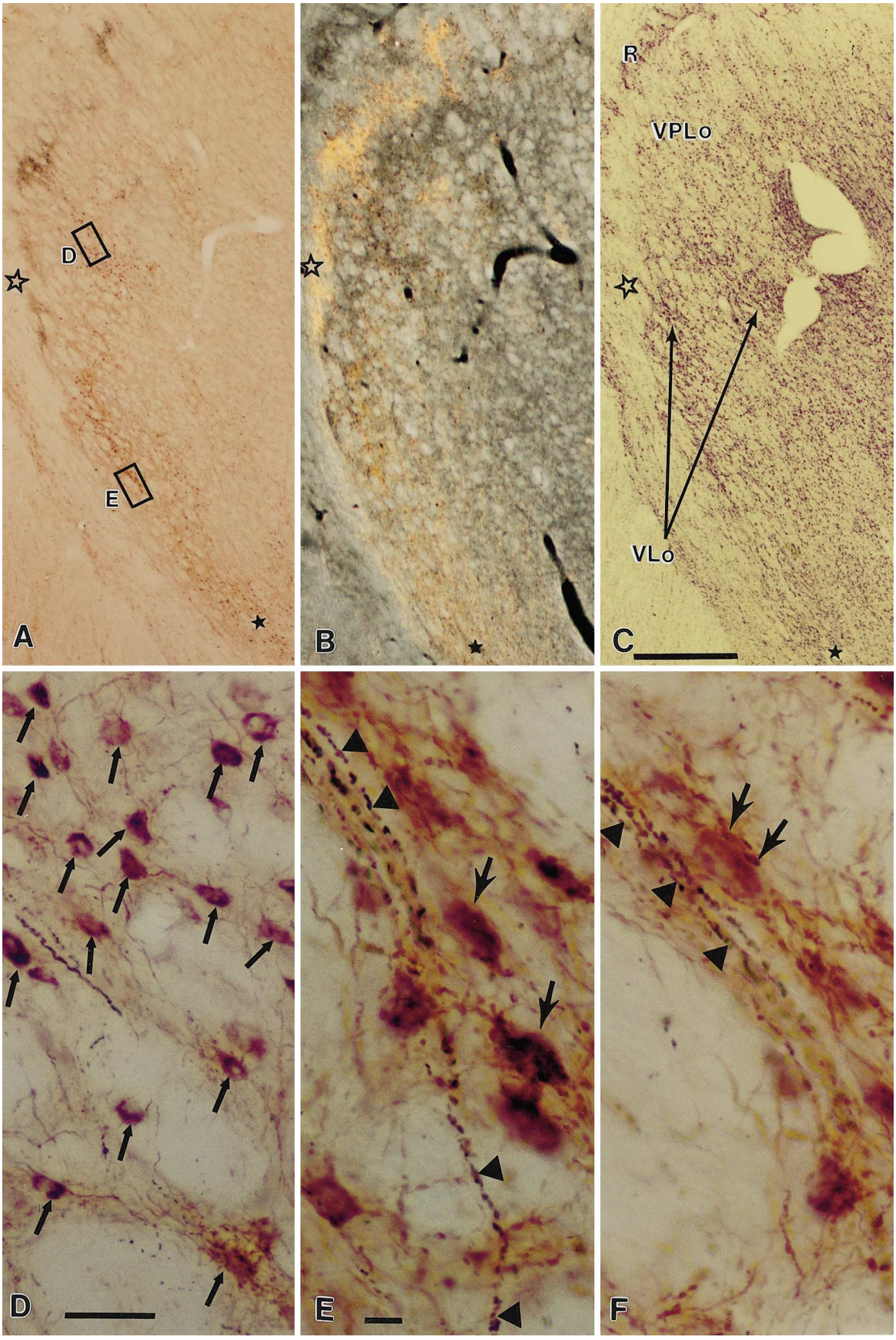
A
D
E
B
C
R
VPLo
VLo
D
E
F

BDA. The BDA anterograde labeling was demonstrated with DAB, which produced homogeneously brown reaction product that filled both axons and varicosities. The SMA thalamocortical cells were most frequently coincident with the pallidal labeling in VApc and VLo (Figs. 4D–F, 5F, 6). However, patchy pallidal anterograde label overlying SMA thalamocortical cells was also found in VLc and in VLm and to minor extent in nucleus X and in VPLo (Fig. 6). The pallidal labeling overlying the CTB-labeled cells was quite dense with axonal varicosities often found closely apposing the cell somata (Fig. 4E, F, 5E, F). Occasionally, BDA-labeled axonal swellings stained brown sometimes gained a purple hue in the triple-stained sections, particularly when viewed at higher magnification (Fig. 5E). However, these labeled BDA fibers could be followed back to the main contingent of pallidal fibers.

The WGA-HRP anterograde labeling from the cerebellar injections was visualized with TMB yielding a granular blue/black precipitate, densely filling fibers and axonal swellings, and resulted in dense patchy labeling extending from VPLo, VLc, and X rostrally to also include VLo and to a lesser extent VApc (Figs. 4A, 5A, 6). Cerebellar fibers were found superimposed over SMA thalamocortical neurons in VLc and transitional zones between VApc, VLo and VPLo. Coincidence of both the SMA cells and cerebellar anterograde label was also observed in X. The SMA thalamocortical cells were densely covered by patchy cerebellothalamic-labeling sometimes obscuring the profile of the labeled cell somata (Fig. 5D). The irregular transitional region between the densely clustered darkly stained cells of VLo and the cell sparse VPLo easily recognizable in Nissl stained material as shown in Figs. 4C, 5C, occasionally contained cerebellothalamic fibers in close proximity to the same SMA thalamocortical cells superimposed upon by pallidothalamic label (Fig. 5E). This arrangement was also noted in the ventral portion of VLo (Fig. 5F) and VPLo and in VLm.

The CTB injections were larger in our additional cases and resulted in more thalamic cell labeling. In these cases, additional retrogradely labeled cells were found in VLo, VPLo, VLc and X. These cells were primarily coincident with pallidal plexuses but overlap with cerebellar label was also noted particularly in VPLo and X.

The sequential histochemical processing used in this study resulted in clearly distinguishable three-color labeling of multiple projection systems. We found the triple-labeling method to be specific for the three tracers and have found no evidence of cross reactivity. The control sections, including the WGA-HRP only series, revealed no false positive staining from the other tracers and the CTB series that was reacted without the primary antisera demonstrated the specificity of the CTB immunostaining. A BDA only control series was not tested since this series would lead to false positive staining due to the presence of the WGA-HRP, which also stains with DAB.

Fig. 4 A series of low power photomicrographs of coronal sections through rostral thalamus from case X. **A**, **B** Bright- and dark-field photomicrographs of a section sequentially reacted for HRP histochemistry using TMB, BDA immunohistochemistry using DAB, and CTB immunohistochemistry using VIP. Note the black patches of WGA-HRP anterograde label, the light brown BDA anterograde label and the purple CTB retrograde cell labeling. Major cytoarchitectonic features at this thalamic level are shown in the a cresyl violet stained section in **C**. *Stars* denote the same blood vessels in **A**–**C**. *Bar* 1.0 mm. *Boxed areas* are shown at higher magnification in **D** and in **E**, **F**. **D** Transitional area between VLo and VPLo containing CTB-labeled cells. *Arrows* denote the purple CTB-labeled cells. *Bar* 50 μm. **E**, **F** At higher magnification. **E** *Arrows* denote the purple CTB-labeled cells surrounded by brown BDA (pallidal)-labeled fibers and plexuses in ventral VLo. *Arrowheads* indicate passing black WGA-HRP (cerebellar) fibers. **F** Note the purple CTB-labeled cells and adjacent BDA-labeled varicosities (*arrows*). *Arrowhead* indicates black WGA-HRP (cerebellar) fibers. *Bar* 10 μm

Discussion

In the present study, we demonstrated coincidence between the SMA thalamocortical neurons and the pallidothalamic and cerebellothalamic territories using a novel combination of three neuroanatomical tracers which permitted the simultaneous observation of dual anterograde projections and retrograde cell labeling. On the basis of this combination of tracers, we provide direct evidence that the SMA thalamocortical neurons receive primarily pallidothalamic input and secondarily cerebellothalamic input.

We combined the retrograde transport of CTB with the anterograde transport of both WGA-HRP and of BDA in a single case and employed sequential histochemical processing utilizing three different chromogens in order to visualize all three tracers in the same section. The observation of all three tracers in a single section permitted direct assessment of interdigitating projection systems and is superior to the more common comparison of adjacent sections treated for different histochemical procedures. In addition, this multiple-labeling paradigm resulted in stable, permanent reaction products. Thus, this method is preferable to neuroanatomical tracing techniques using multiple-fluorescent dyes that quench and fade upon exposure to excitation wavelengths. One drawback inherent to the triple-labeling paradigm is the difficulty in clearly distinguishing multiple projections when one projection system is especially dense. Dense labeling from a single projection system may effectively mask the second or third label. For example, the cerebellothalamic projection is massive and in some regions, the blue-black WGA-HRP labeling almost completely covered the purple CTB-labeled cells, making it difficult to clearly distinguish and differentiate the labeled cells (Fig. 5 D). However, careful microscopic examination using higher magnifications revealed the secondary or tertiary labeling. In addition, background staining levels were higher in the triple reaction sections than in either the single- or double-reacted sections. In some cases, the VIP incubation period

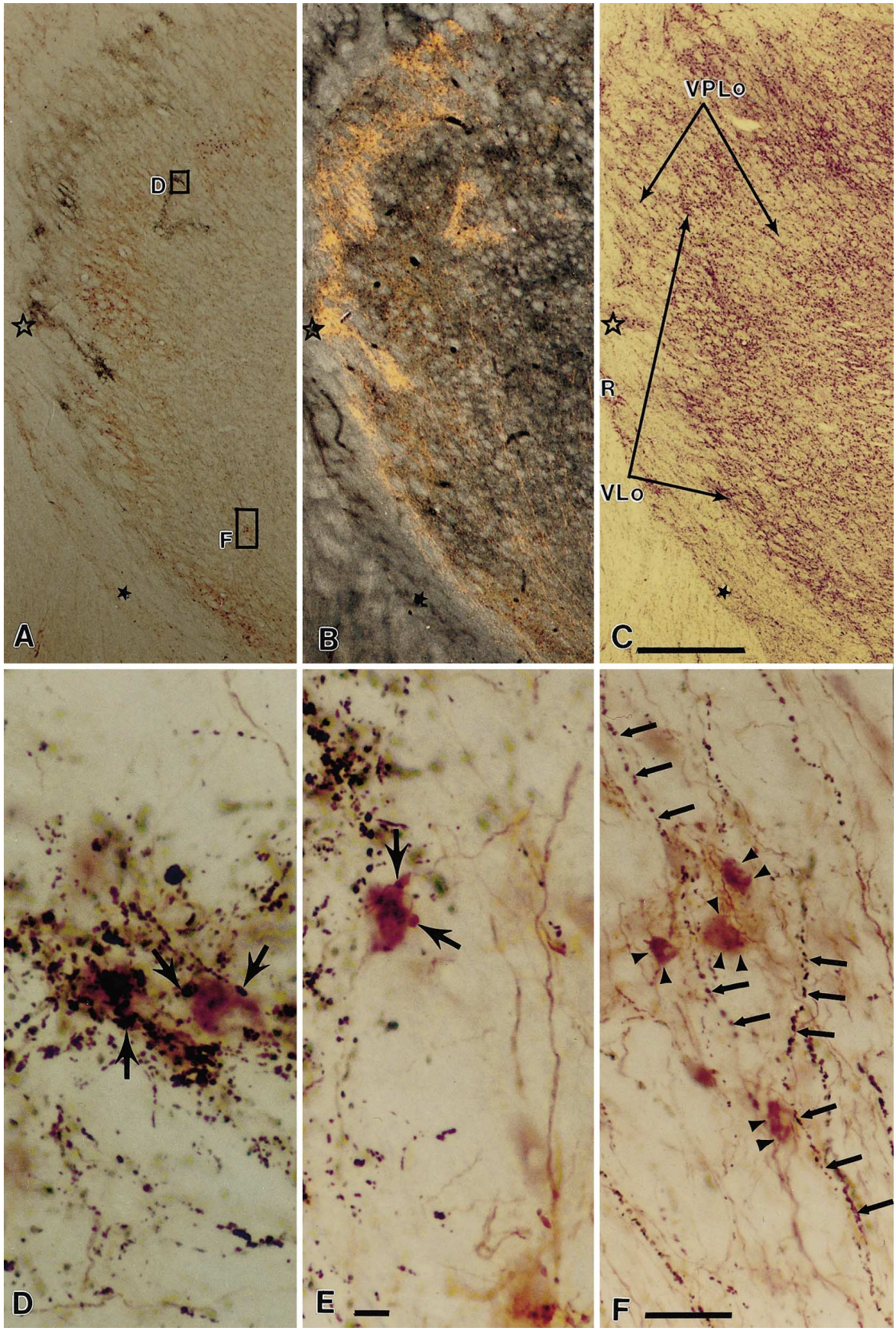
D
F
A
B
VPLo
R
VLo
C
D
E
F

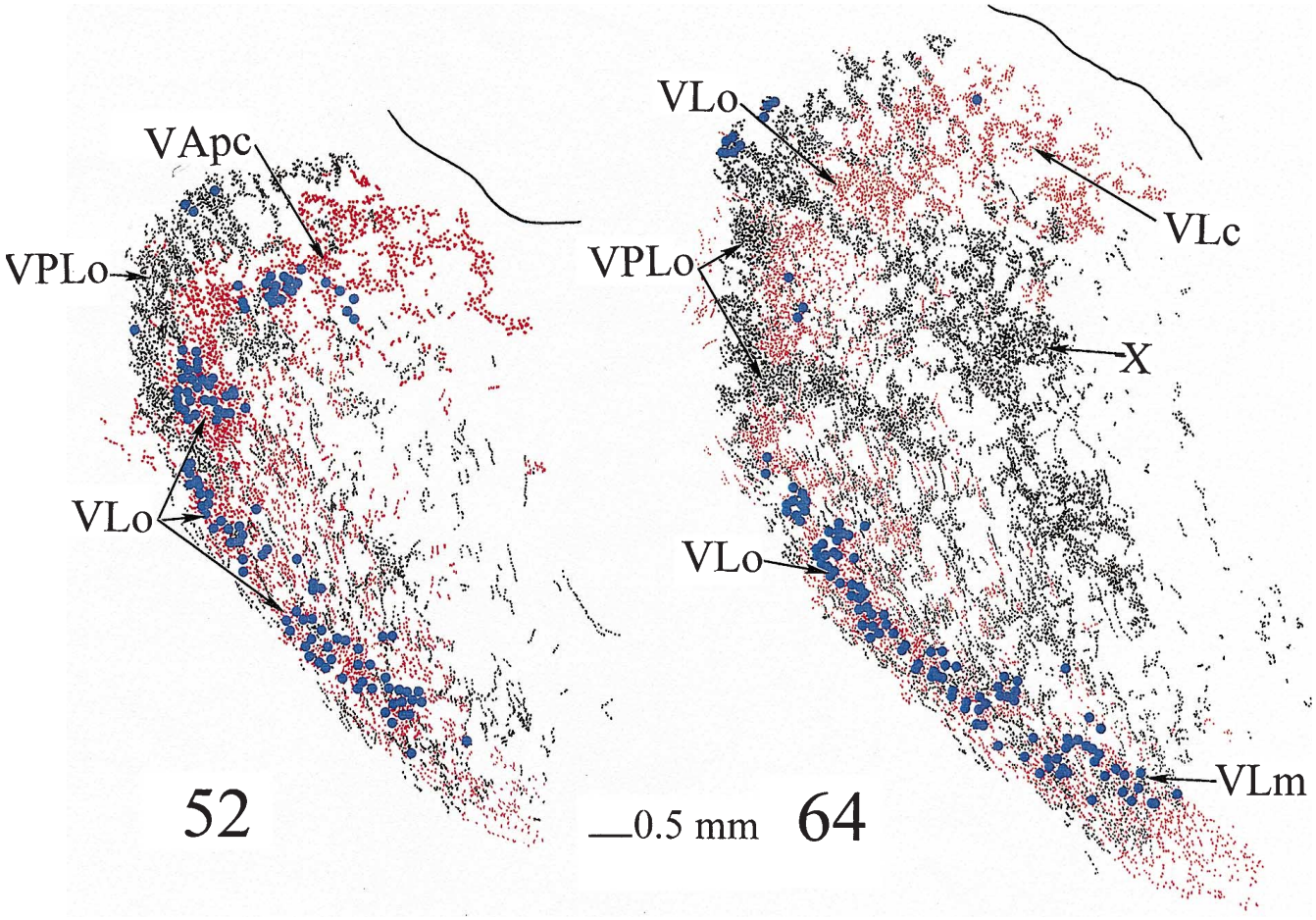

Fig. 6 Line drawings of coronal sections through the primate thalamus showing the distribution of pallidothalamic and cerebellothalamic anterograde label and the location of the SMA thalamocortical projection neurons in case X. *Blackened stippling* indicates the WGA-HRP-anterograde label following the injections into the contralateral cerebellar nuclei. *Red stippling* indicates labeling following the BDA injections into GPi. *Blue dots* indicate the SMA thalamocortical projection neurons following the CTB injections into the forelimb representation in SMA. Note the coincidence of the SMA cells with pallidal label primarily in VApc and VLo in section 52 and VLo in section 64. Some SMA cells coincided with cerebellothalamic label in VPLo in both sections 52 and 64. Transitional areas between VApc, VLo and VPLo contained SMA cells that overlapped with either pallidal or cerebellar label

◀ **Fig. 5** A series of low-power photomicrographs of coronal sections through mid-thalamus from case X. **A**, **B** Bright- and darkfield photomicrographs of a section sequentially reacted for all three labels. Note the black patches of WGA-HRP anterograde label, the brown BDA label and the purple CTB retrograde cell labeling. Major cytoarchitectonic features at this thalamic level are shown in the cresyl violet-stained section in **C**. Note the cell islands containing darkly stained cells characteristic of VLo blending into the cell sparse VPLo. *Stars* denote the same blood vessels in **A**–**C**. *Bar* 1.0 mm. *Boxed areas* are shown in higher magnification in **D**–**F**. **D** A dense patch of black WGA-HRP (cerebellar) label (*arrows*) overlapping purple CTB-labeled cells in a cell sparse island of VPLo. **E** BDA (pallidal) labeled varicosities (*arrows*) closely apposed to a purple CTB cell in a patch of label immediately adjacent to **D**. Note the close proximity of the black WGA-HRP (cerebellar) label. *Bar* 10 μm. **F** Lower magnification photomicrograph through ventral VLo showing purple CTB-labeled cells surrounded by brown BDA (pallidal) fibers and plexuses (*arrowheads*). *Small arrows* denote passing black WGA-HRP (cerebellar) axons. *Bar* 50 μm

was shortened to as little as 5 min and required modification according to each individual case in order to minimize background staining.

This combination of tracers directly revealed details of afferent and efferent connectivity. At the light microscopic level, the WGA-HRP injections and the BDA injections resulted in dense labeling of fibers and swellings. Thalamocortical neurons labeled with CTB stained intensely purple. Occasionally, we also observed anterograde CTB reaction product that appeared as a light purple dusting. Both retrograde and anterograde transport of CTB have been previously reported (Luppi et al. 1990; Bruce and Grofova 1992). We also observed that some of the labeled BDA or WGA-HRP swellings were closely apposed to the CTB retrogradely labeled cells. These observations are suggestive of synaptic contacts although electron microscopic verification is lacking in the present study. In this regard, it is of interest that Wouterlood and Gronewegen (1985) reported that similarly labeled axonal varicosities are the light microscopic representation of synaptic axonal terminals as seen in the electron microscope.

In the present study, we found that the SMA thalamocortical neurons were primarily coincident with the pallidothalamic territory and secondarily with the cerebellothalamic territory. Our findings support the results of a number of single-labeling studies (Schell and Strick 1984; Darian-Smith et al. 1990; Shindo et al. 1995) as

well as more recent multiple labeling studies (Tokuno et al. 1992; Rouiller et al. 1994) that reported a strong linkage between the SMA-projecting thalamic neurons and pallidal inputs. In addition, we provided direct evidence that the cerebellothalamic territory overlapped the SMA projection neurons. These results support the indirect observations of transthalamic afferents from the cerebellum to SMA reported by Wiesendanger and Wiesendanger (1985b) and by Roullier et al. et al. (1994).

In a previous study (Sakai et al. 1996), we described an anterior-posterior gradient with respect to pallidothalamic and cerebellothalamic projections. The pallidothalamic territory was densest anteriorly in VApc, VLo, VLc and diminished posteriorly with minor projections to VLPo and X, whereas the cerebellothalamic territory was densest posteriorly from VPLo, X and VLc and diminished anteriorly with minor projections to VLo and VApc. Our present data suggests that the band of SMA projection neurons are superimposed on this gradient. In this report, we found patches of pallidothalamic label overlapping the SMA projection neurons in VApc and VLo as well as occasionally in VLPo, nucleus X and VLc. In addition, the cerebellothalamic label primarily overlapped the SMA projection neurons in VLo and VLc. Occasional overlap of SMA projection cells and cerebellothalamic label was found in nucleus X and VLPo. Taken together, these observations suggest that the SMA receives mixed and weighted thalamic input from the basal ganglia and cerebellum.

Although our findings are at odds with the prevailing view of segregated and parallel pathways (Schell and Strick 1984; Alexander et al. 1986), the notion of weighted thalamic input to a specific cortical area is not new. Kievit and Kuypers (1977) first described a band-like distribution of thalamic projection neurons to specific cortical targets on the basis of a HRP retrograde labeling study. In addition, on the basis of the retrograde transport of multiple fluorescent dyes, Darian-Smith et al. (1990) have hypothesized that specific subdivisions of the sensorimotor cortex receive mixed afferents originating from the cerebellum, basal ganglia and spinal cord. Since the band of retrograde cell labeling transversed thalamic nuclear boundaries, it was suggested that separate cortical subdivisions receive multiple thalamic sources (Kievit and Kuypers 1977; Darian-Smith et al. 1990). Our results confirm and extend these findings by directly demonstrating that the input to the SMA is not only derived from a band of cells arising from a multiple thalamic nuclei, but also, that these same thalamic nuclei are the recipients of patchy and focal input from GPi and the cerebellum.

An anatomical substrate consisting of interdigitating pallidal and cerebellar patches overlapping the SMA projection neurons may partially provide the basis for both the complexity of neuronal responses reported for the SMA in the behaving monkey (Georgopoulos 1991; Tanji 1994) as well as account for the similarities in the response properties between the SMA and MI (Tanji and Kurata 1982; Alexander and Crutcher 1990a, b; Shibasaki et al. 1993), a cortical region known to receive strong transthalamic cerebellar input with secondary input from the GPi (Yamamoto et al. 1983; Nambu et al. 1988, 1991; Holsapple et al. 1991; Jinnai et al. 1993; Rouiller et al. 1994; Inase and Tanji 1995; Sakai et al. 1995). Moreover, neural circuits consisting of mixed inputs may contribute to a more flexible substrate subject to modification. In this regard, it is of interest that Aizawa et al. (1991) have noted cellular changes in the supplementary motor area as a result of motor learning.

Acknowledgements We express our sincere appreciation to Mrs. Michi Seo for her excellent technical assistance and Drs. Irena Grofova, the late Duke Tanaka, Jr. and Iwona Stepniewska for their critical comments. This research was supported in part by Grants-in-Aid for Scientific Research from the Japanese Ministry of Education, Science and Culture (06NP0101).

References

Agostino R, Berardelli A, Formicia A, Accornero N, Manfredi M (1992) Sequential arm movements in patients with Parkinson's disease, Huntington's disease and dystonia. Brain 115:1481–1495

Aizawa H, Inase M, Mushiake H, Shima K, Tanji J (1991) Reorganization of activity in the supplementary motor area associated with motor learning and functional recovery. Exp Brain Res 84:668–671

Alexander GE, Crutcher MD (1990a) Neural representations of the target (goal) of visually guided arm movements in three motor areas in the monkey. J Neurophysiol 64:164–178

Alexander GE, Crutcher MD (1990b) Preparation for movement: neural representations of intended direction in three motor areas of the monkey. J Neurophysiol 64:133–150

Alexander GE, DeLong MR, Strick PL (1986) Parallel organization of functionally segregated circuits linking basal ganglia and cortex. Ann Rev Neurosci 9:357–381

Asanuma C, Thach WT, Jones EG (1983) Distribution of cerebellar terminations and their relation to other afferent terminations in the ventral lateral thalamic region of the monkey. Brain Res Rev 286:237–265

Benecke R, Rothwell JC, Dick JPR, Day BL, Marsden CD (1986) Performance of simultaneous movements in patients with Parkinson's disease. Brain 109:739–757

Brandt HM, Apkarian AV (1992) Biotin-dextran: a sensitive anterograde tracer for neuroanatomic studies in rat and monkey. J Neurosci Methods 45:35–40

Brinkman C (1984) Supplementary motor area of the monkey's cerebral cortex: short- and long-term deficits after unilateral ablations and effects of subsequent callosal section. J Neurosci 4:918–929

Bruce K, Grofova I (1992) Notes on a light and electron microscopic double-labeling method combining anterograde tracing with *Phaseolus vulgaris* leucoagglutinin and retrograde tracing with cholera toxin subunit B. J Neurosci Methods 45:23–33

Darian-Smith C, Darian-Smith I, Cheema SS (1990) Thalamic projections to sensorimotor cortex in the macaque monkey: use of multiple retrograde fluorescent tracers. J Comp Neurol 299:17–46

DeLong M (1971) Activity of pallidal neurons during movements. J Neurophysiol 34:414–427

DeVito JL, Anderson ME (1982) An autoradiographic study of efferent connections of the globus pallidus in *Macaca mulatta*. Exp Brain Res 46:106–117

Dolleman-Van der Weel MJ, Wouterlood FG, Witter MP (1994) Multiple anterograde tracing combining *Phaseolus vulgaris* leucoagglutinin with rhodamine and biotin-conjugated dextran amine. J Neurosci Methods 51:9–21

Dum RP, Strick PL (1991) The origin of corticospinal projections from the premotor areas in the frontal lobe. J Neurosci 11:667–689

Flowers KA (1978) Lack of prediction in the motor behavior in Parkinsonism. Brain 101:35–52

Georgopoulos AP (1991) Higher order motor control. Ann Rev Neurosci 14:361–377

Goldberg G (1985) Supplementary motor area structure and function: review and hypothesis. Behav Brain Sci 8:567–616

Halsband U, Ito N, Tanji J, Freund H-J (1993) The role of premotor cortex and the supplementary motor area in the temporal control of movement in man. Brain 116:243–266

Holsapple JW, Preston JB, Strick PL (1991) The origin of thalamic inputs to the "hand" representation in the primary motor cortex. J Neurosci 11:2644–2654

Inase M, Tanji J (1995) Thalamic distribution of projection neurons to the primary motor cortex relative to afferent terminal fields from the globus pallidus in the macaque monkey. J Comp Neurol 353:415–426

Inase M, Sakai ST, Tanji J (1996) Overlapping corticostriatal projections from the supplementary motor area and the primary motor cortex in the macaque monkey: an anterograde double labeling study. J Comp Neurol 373:283–296

Jinnai K, Nambu A, Tanibuchi I, Yishida S (1993) Cerebello- and pallido-thalamic pathways to areas 6 and 4 in the monkey. Stereotact Funct Neurosurg 60:70–79

Kievit J, Kuypers HGJM (1977) Organization of the thalamocortical connections to the frontal lobe in the rhesus monkey. Exp Brain Res 29:299–322

Kim R, Nakano K, Jayaraman A, Carpenter MB (1976) Projections of the globus pallidus and adjacent structures: an autoradiographic study in the monkey. J Comp Neurol 169:263–290

Kuo J-S, Carpenter MB (1973) Organization of pallidothalamic projections in the rhesus monkey. J Comp Neurol 151:201–236

Kusama T, Mabuchi M (1970) Stereotaxic atlas of the brain of *Macaca fuscata*. University of Tokyo Press, Tokyo

Luppi P-H, Fort P, Jouvet M (1990) Iontophoretic application of unconjugated cholera toxin B subunit (CTb) combined with immunohistochemistry of neurochemical substances: a method for transmitter identification of retrogradely labeled neurons. Brain Res 534:209–224

Luppino G, Matelli M, Camarda RM, Gallese V, Rizzolatti G (1991) Multiple representations of body movements in mesial area 6 and the adjacent cingulate cortex: an intracortical microstimulation study in the macaque monkey. J Comp Neurol 311:463–482

Luppino G, Matelli M, Camarda RM, Rizzolatti G (1993) Corticocortical connections of area F3 (SMA-proper) and area F6 (Pre-SMA) in the macaque monkey. J Comp Neurol 338:114–140

Matelli M, Luppino G, Rizzolatti G (1991) Architecture of superior and mesial area 6 and the adjacent cingulate cortex in the macaque monkey. J Comp Neurol 311:445–462

Murray EA, Coulter JD (1981) The organization of corticospinal neurons in the monkey. J Comp Neurol 195:339–365

Nambu A, Yoshida S, Jinnai K (1988) Projection on the motor cortex of thalamic neurons with pallidal input in the monkey. Exp Brain Res 71:658–662

Nambu A, Yoshida S, Jinnai K (1991) Movement-related activity of thalamic neurons with input from the globus pallidus and projection to the motor cortex in the monkey. Exp Brain Res 84:279–284

Olszewski J (1952) The thalamus of the *Macaca mulatta.* Karger, Basel

Olucha F, Martinex-Garcia F, Lopez-Carcia C (1985) A new stablizing agent for the tetramethyl benzidine (TMB) reaction product in the histochemical detection of horseradish peroxidase (HRP). J Neurosci Methods 1:131–138

Roland PE, Larsen B, Lassen NA, Shinhøj E (1980) Supplementary motor area and other cortical areas in organization of voluntary movement in man. J Neurophysiol 43:118–136

Rouiller E, Liang F, Babalian A, Moret V, Wiesendanger M (1994) Cerebellothalamocortical and pallidothalamocortical projections to the primary and supplementary motor cortical areas: a multiple tracing study in macaque monkeys. J Comp Neurol 345:185–213

Rye DB, Saper CB, Wainer BH (1984) Stabilization of the tetramethyl benzidine (TMB) reaction product: application for retrograde and anterograde tracing and combination with immunohistochemistry. J Histochem Cytochem 32:1145–1153

Sakai ST, Inase M, Tanji J (1995) Organization of the pallidothalamocortical and cerebellothalamocortical pathway in the monkey: a multiple retrograde and anterograde labeling study. Soc Neurosci Abstr 25:410

Sakai ST, Inase M, Tanji J (1996) Comparison of cerebellothalamic and pallidothalamic projections in the monkey (*Macaca fuscata*): a double anterograde labeling study. J Comp Neurol 368:215–228

Schell GR, Strick PL (1984) The origin of thalamic inputs to the arcuate premotor and supplementary motor areas. J Neurosci 5:539–560

Shibasaki H, Sadato N, Lyshkow H, Yonekura Y, Honda M, Nagamine T, Suwazono S, Magata Y, Ikeda A, Miyazaki M, Fukuyama H, Asato R, Konishi J (1993) Both primary motor cortex and supplementary motor area play an important role in complex finger movement. Brain 116:1387–1398

Shindo K, Shima K, Tanji J (1995) Spatial distribution of thalamic projections to the supplementary motor area and the primary motor cotex: a retrograde multiple – labeling study in the macaque monkey. J Comp Neurol 357:98–116

Tanji J (1994) The supplementary motor area in the cerebral cortex. Neurosci Res 19:251–268

Tanji J, Kurata K (1982) Comparison of movement-related activity in two cortical areas in primates. J Neurophysiol 48: 633–653

Tanji J, Shima K (1994) Role for supplementary motor area cells in planning several movements ahead. Nature 371:413–416

Tanji J, Taniguchi K, Saga T (1980) Supplementary motor area: neuronal response to motor instructions. J Neurophysiol 43:60–68

Tokuno H, Kimura M, Tanji J (1992) Pallidal inputs to thalamocortical neurons projecting to the supplementary motor area: an anterograde and retrograde double labeling study in the Macaque monkey. Exp Brain Res 90:635–638

Veenman CL, Reiner A, Honig MG (1992) Biotinylated dextran amine as an anterograde tracer for single- and souble-labeling studies. J Neurosci Methods 41:239–254

Wiesendanger M, Wiesendanger R (1985a) The supplementary motor area in the light of recent investigations. Exp Brain Res 9:382–392

Wiesendanger R, Wiesendanger M (1985b) Cerebello-cortical linkage in the monkey as revealed by transcellular labeling with the lectin wheat germ agglutinin conjugated to the marker horseradish peroxidase. Exp Brain Res 59:105–117

Wouterlood FG, Groenewegen HJ (1985) Neuroanatomic tracing by use of *Phaseolus vulgaris* leucoagglutinin (PHA-L): electron microscopy of PHA-L filled neuronal somata, dendrites, axons and axonal terminals. Brain Res 326:188–191

Yamamoto T, Hassler R, Huber C, Wagner A, Sasaki K (1983) Electrophysiologic studies on the pallido- and cerebellothalamic projections in squirrel monkeys (*Saimiri sciureus*). Exp Brain Res 51:77–87

Zhou M, Grofova I (1995) The use of peroxidase substrate Vector VIP in electron microscopic single and double antigen localization. J Neurosci Methods 62:149–158